

Perturbative predictions for color superconductivity on the lattice

Takeru Yokota,^{a,b,*} Yuhma Asano,^c Yuta Ito,^d Hideo Matsufuru,^{e,f} Yusuke Namekawa,^g Jun Nishimura,^{e,f} Asato Tsuchiya^h and Shoichiro Tsutsuiⁱ

^a*Interdisciplinary Theoretical and Mathematical Sciences Program (iTHEMS), RIKEN, Wako, Saitama 351-0198, Japan*

^b*Institute for Solid State Physics, The University of Tokyo, Kashiwa, Chiba 277-8581, Japan*

^c*Faculty of Pure and Applied Sciences, University of Tsukuba, 1-1-1 Tennodai, Tsukuba, Ibaraki 305-8577 Japan*

^d*National Institute of Technology, Tokuyama College, Gakuendai, Shunan, Yamaguchi 745-8585, Japan*

^e*High Energy Accelerator Research Organization (KEK), 1-1 Oho, Tsukuba, Ibaraki 305-0801, Japan*

^f*School of High Energy Accelerator Science, Graduate University for Advanced Studies (SOKENDAI), 1-1 Oho, Tsukuba, Ibaraki 305-0801, Japan*

^g*Department of Physics, Kyoto University, Kyoto 606-8502, Japan*

^h*Department of Physics, Shizuoka University, 836 Ohya, Suruga-ku, Shizuoka 422-8529, Japan*

ⁱ*Quantum Hadron Physics Laboratory, RIKEN Nishina Center, Wako, Saitama 351-0198, Japan*

E-mail: takeru.yokota@riken.jp

We develop a new method to investigate color superconductivity (CSC) on the lattice based on the Thouless criterion, which amounts to solving the linearized gap equation without imposing any ansatz on the structure of the Cooper pairs. We perform explicit calculations at the one-loop level with the staggered fermions on a $8^3 \times 128$ lattice and the Wilson fermions on a $4^3 \times 128$ lattice, which enables us to obtain the critical $\beta (= 6/g^2)$ as a function of the quark chemical potential μ , below which the CSC phase is expected to appear. The obtained critical β has sharp peaks at the values of μ corresponding to the discretized energy levels of quarks similarly to what was observed in previous studies on simplified effective models. From the solution to the linearized gap equation, one can read off the flavor and spatial structures of the Cooper pairs at the critical β . In the case of massless staggered fermion, in particular, we find that the chiral U(1) symmetry of the staggered fermions is spontaneously broken by the condensation of the Cooper pairs.

*The 38th International Symposium on Lattice Field Theory, LATTICE2021 26th-30th July, 2021
Zoom/Gather@Massachusetts Institute of Technology*

¹RIKEN-iTHEMS-Report-21, RIKEN-QHP-505, KEK-TH-2360, KUNS-2897

*Speaker

1. Introduction

The QCD phase diagram is expected to have a rich structure, whose elucidation is one of the biggest goals in high energy physics. While the first-principles studies of the dense QCD matter is known to be extremely difficult due to the notorious sign problem, there are various methods that have been developed in recent years to circumvent this problem. In particular, the complex Langevin method [1, 2] has been applied to lattice QCD at finite density with promising results; see Ref. [3] and references therein.

In fact, the QCD phase diagram can be investigated in the high density regime by perturbation theory thanks to the asymptotic freedom. In particular, it is expected that the color superconductivity (CSC) [4–8] occurs in the cold dense region considering that the color-anti-triplet channel of the potential induced by one-gluon exchange is attractive. Qualitative properties of the CSC such as the scaling of the gap function with respect to the coupling constant have been discussed based on perturbative QCD [9].

Perturbative studies are expected to be useful not only in exploring the QCD phase diagram at high density but also in providing predictions for first-principles calculations in the cold dense region, which seem to be quite promising [10]. While quantitative predictions on the parameter region in which the CSC occurs were discussed in simplified effective models such as the Nambu–Jona-Lasinio-like model [7, 8], there have been no such works in QCD. One of the reasons for this is that one has to solve a nonlinear functional equation known as the gap equation, which is extremely difficult, in particular, without imposing some ansatz on the gap function.

In this paper, we investigate the CSC by solving the gap equation on the lattice without imposing any ansatz on the structure of the gap function describing the condensation of the Cooper pairs. This is possible since the gap equation is reduced on the lattice to a finite number of coupled equations. Further simplification of the gap equation is achieved by focusing on the critical point so that the gap equation can be linearized. The condition for the linearized gap equation to have a nontrivial solution is well known in the condensed matter physics as the Thouless criterion, but to our knowledge, this is the first time that it was applied to the CSC in QCD.

Thus, our method enables us to provide a quantitative prediction on the parameter region of the CSC by calculating the critical coupling $\beta = 6/g^2$, which we denote as β_c in what follows, as a function of the quark chemical potential for the staggered and Wilson fermions. The results for β_c show peak structure as a function of the chemical potential, which is due to the discretized energy levels of quarks in a finite volume. We also investigate the structure of the Cooper pairs at β_c from the solution to the linearized gap equation in the case of massless staggered fermions. From the results for scalar and pseudo-scalar condensates, we find that the chiral U(1) symmetry is broken spontaneously. The spatial structure of the Cooper pairs, on the other hand, exhibits behaviors consistent with the BCS theory of superconductivity.

The rest of this paper is organized as follows. In Section 2, we present our general formalism for the CSC. In Section 3, we show our numerical results for β_c in the case of staggered fermions, followed by Section 4, where we investigate the structure of the Cooper pairs at the critical point in the massless case. In particular, we identify the flavor and spatial structures of the Cooper pairs and discuss the spontaneous breaking of chiral U(1) symmetry. In Section 5, we present our results for β_c in the case of Wilson fermions. Section 6 is devoted to a conclusion.

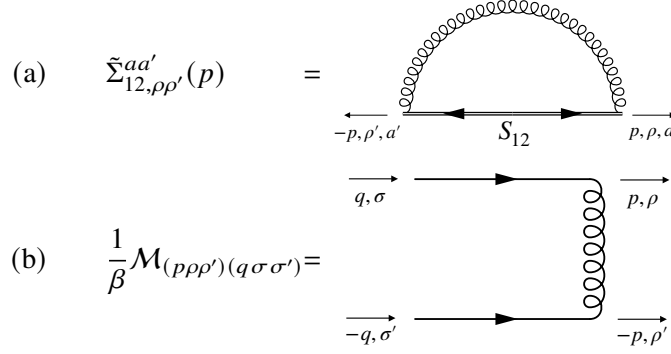


Figure 1: Diagrammatic representation of (a) the gap equation for $\tilde{\Sigma}_{12,\rho\rho'}^{aa'}(p)$ and (b) $\mathcal{M}_{(p\rho\rho')(q\sigma\sigma')}$. The coiled and solid lines stand for the gluon propagator and the free fermion propagator $\tilde{D}_{\rho\rho'}^{-1,aa'}(p)$, respectively.

2. General formalism for CSC on the lattice

Since we are going to investigate CSC on the lattice for staggered and Wilson fermions, here we describe a general formalism, which is applicable to both cases. We introduce a fermion field $\psi_\rho^a(n)$, where n is the label of sites on the lattice, and a is the color index. The index ρ represents the internal degrees of freedom other than color such as the flavor index and the spinor index collectively. We also introduce the conjugate field $\bar{\psi}_\rho^a(n)$.

In order to investigate the condensate of Cooper pairs, we use the Nambu-Gorkov formalism, in which one introduces the Nambu basis $\Psi_\rho^a(n) = (\psi_\rho^a(n), \bar{\psi}_\rho^a(n))^t$ [4, 6, 11]. Assuming that the lattice translational symmetry is not spontaneously broken, it is convenient to work with the momentum representation since two-point correlation functions are diagonalized with respect to momenta owing to the momentum conservation. The propagator for the Nambu basis $\tilde{\mathbf{S}}_{\rho\rho'}^{aa'}(p)$ in the momentum representation can be represented by a 2×2 matrix, which satisfies the Dyson equation

$$\tilde{\mathbf{S}}_{\rho\rho'}^{-1,aa'}(p) = \tilde{\mathbf{D}}_{\rho\rho'}^{aa'}(p) + \tilde{\Sigma}_{\rho\rho'}^{aa'}(p), \quad (1)$$

where $\tilde{\mathbf{D}}_{\rho\rho'}^{aa'}(p)$ is the inverse free propagator defined by $\tilde{\mathbf{D}}_{\rho\rho'}^{aa'}(p) = \text{diag}(\tilde{D}_{\rho\rho'}^{aa'}(p), -\tilde{D}_{\rho\rho'}^{aa'}(-p))$ with $\tilde{D}_{\rho\rho'}^{aa'}(p)$ being the inverse free propagator for $\psi_\rho^a(n)$ and $\tilde{\Sigma}_{\rho\rho'}^{aa'}(p)$ being the self-energy defined as

$$\tilde{\Sigma}_{\rho\rho'}^{aa'}(p) = \begin{pmatrix} \tilde{\Sigma}_{11,\rho\rho'}^{aa'}(p) & \tilde{\Sigma}_{12,\rho\rho'}^{aa'}(p) \\ \tilde{\Sigma}_{21,\rho\rho'}^{aa'}(p) & \tilde{\Sigma}_{22,\rho\rho'}^{aa'}(p) \end{pmatrix}. \quad (2)$$

A nonvanishing off-diagonal part of the self-energy $\tilde{\Sigma}_{12(21),\rho\rho'}^{aa'}(p)$ corresponds to the appearance of pair condensate, which is crucial for the CSC, while the diagonal part is considered as higher-order contributions in our calculation, which is neglected in what follows.

At the one-loop level, the self-consistency equation for $\tilde{\Sigma}_{12,\rho\rho'}^{aa'}(p)$ or the gap equation is given by Fig. 1 (a). The gap equation for the other off-diagonal part $\tilde{\Sigma}_{21,\rho\rho'}^{aa'}(p)$ need not be considered since it gives the same results as the one for $\tilde{\Sigma}_{12,\rho\rho'}^{aa'}(p)$. While one can obtain $\tilde{\Sigma}_{12,\rho\rho'}^{aa'}(p)$ in principle

by solving the gap equation together with the Dyson equation (1), it does not seem to be feasible to do so in practice without having a natural ansatz to impose on $\tilde{\Sigma}_{12}(p)$ for arbitrary parameters. Instead, we focus on the critical point at which $\tilde{\Sigma}_{12}(p) \rightarrow 0$ assuming a second-order phase transition. This reduces the gap equation to a linear equation, which can be solved without imposing any ansatz on $\tilde{\Sigma}_{12}(p)$. Here we consider the color anti-symmetric component $\sum_{ab} \epsilon_{abc} \tilde{\Sigma}_{12,\rho\rho'}^{ab}(p)$, for which the interaction is attractive and hence the Cooper instability is expected. Since a different choice of c simply leads to the same equation, we choose $c = 3$ without loss of generality and define $\tilde{\Sigma}_{12(p\rho\rho')}^{(-)} = \sum_{ab} \epsilon_{ab3} \tilde{\Sigma}_{12,\rho\rho'}^{ab}(p)$, which satisfies the linearized gap equation

$$\sum_{q\sigma\sigma'} \mathcal{M}_{(p\rho\rho')(q\sigma\sigma')} \tilde{\Sigma}_{12(q\sigma\sigma')}^{(-)} = \beta \tilde{\Sigma}_{12(p\rho\rho')}^{(-)}. \quad (3)$$

We have introduced $\beta = 2N_c/g^2$, where g is the gauge coupling constant with $N_c = 3$ in the case at hand. The matrix $\mathcal{M}_{(p\rho\rho')(q\sigma\sigma')}$ is independent of β , and it is given diagrammatically in Fig. 1 (b). From Eq. (3), one finds that the largest eigenvalue of \mathcal{M} gives the critical point

$$\beta_c = \lambda_{\max}[\mathcal{M}], \quad (4)$$

which determines the boundary of the normal and superconducting phases. The eigenvector $\tilde{\Sigma}_{12(p\rho\rho')}^{(-)}$ corresponding to the largest eigenvalue, on the other hand, tells us the structure of the Cooper pairs at the critical point. Such a condition for the critical point is equivalent to the condition for the divergence of the T-matrix, which is well known as the Thouless criterion [12] in condensed matter physics. Since the size of the matrix \mathcal{M} is finite for a finite lattice, we can calculate the largest eigenvalue $\lambda_{\max}[\mathcal{M}]$ and the corresponding eigenvector numerically by the standard power iteration method.

3. Critical coupling for the staggered fermions

Let us first consider staggered fermions and present our numerical results for β_c as a function of the quark chemical potential μ defined in lattice units. Note that our calculation is valid at weak coupling, which implies that the results are reliable if $\beta_c \gg 1$. We find that this is possible when the aspect ratio L_s/L_t is sufficiently small, where L_s and L_t represent the spatial and temporal extents of the lattice, respectively.

Figure 2 shows the result for an $8^3 \times 128$ lattice and the quark mass $m = 0$ and 0.1 in lattice units. We also plot the number of quarks N_q in the same figure for $m = 0$ in the free case. One can see that the peaks of β_c appear at the values of μ for which N_q jumps from one plateau to another. This can be understood theoretically as follows. Let us note first that the energy levels of free quarks $E(\mathbf{p}) = \sinh^{-1} \sqrt{\sum_{i=1}^3 \sin^2 p_i + m^2}$ are discretized since the momentum \mathbf{p} is discretized in a finite volume. When the chemical potential μ goes beyond an energy level $E(\mathbf{p})$, N_q jumps because the number of momentum modes below the Fermi sphere increases. Since there are momentum modes near the Fermi surface in this situation, the Cooper pairs are easy to form, and hence the critical β_c has a peak at the same μ . This understanding is supported also by the result for $m = 0.1$ in Fig. 2, where we observe that the peaks shift in accord with the shift of the energy levels. Thus we find that the CSC region is suppressed when the chemical potential is not close to any of the energy levels of

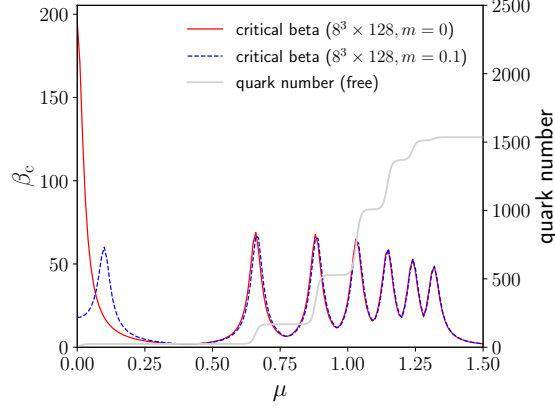


Figure 2: The critical coupling β_c is plotted as a function of μ on an $8^3 \times 128$ lattice using the staggered fermions with $m = 0$ (red solid line) and $m = 0.1$ (blue dashed line). The regions above and below these lines correspond to the normal and color-superconducting phases, respectively. The gray solid line represents the quark number for $m = 0$ in the free case.

quarks, as has been also observed in the Nambu–Jona-Lasinio-like model [13]. The peak at $\mu \sim 0$ is considered to be a finite-size artifact since the Cooper pairs in this case are formed by quarks and anti-quarks with $\mathbf{p} = \mathbf{0}$, whose density actually vanishes in the infinite volume limit.

4. Structure of the Cooper pairs for the staggered fermions

As we mentioned in Section 2, the structure of the Cooper pairs can be read off from the eigenvector $\tilde{\Sigma}_{12(p\rho\rho')}^{(-)}$ corresponding to $\lambda_{\max}[\mathcal{M}]$. For that, we rewrite $\tilde{\Sigma}_{12(p\rho\rho')}^{(-)}$ in Eq. (1) into the anomalous correlation function of the four-flavor Dirac fermion fields in the coordinate space using the relation between the staggered and Dirac fermions [14] and performing the Fourier transformation. While our calculation is applicable to the Cooper pairs in any irreducible representations of the Lorentz group, let us focus, for simplicity, on the scalar (s) and pseudo scalar (ps) condensates given as

$$K_{s(\text{ps})}^{fg}(n) = \sum_{ab} \epsilon_{ab3} \langle {}^t\psi^{a,f}(n) \mathcal{O}_{s(\text{ps})} \psi^{b,g}(0) \rangle. \quad (5)$$

Here $\psi^{a,f}(n)$ represents the Dirac fermion field on the coarse lattice at a site N with the color index a and the flavor index f . We have also introduced $\mathcal{O}_s = \gamma_5 C$ and $\mathcal{O}_{\text{ps}} = C$, where $\gamma_5 = \gamma_1 \gamma_2 \gamma_3 \gamma_4$ and the charge conjugation operator $C = \gamma_2 \gamma_4$ are defined in terms of the Euclidian Dirac gamma matrices γ_μ . Note that the overall normalization of $K_{s(\text{ps})}^{fg}(n)$ is irrelevant since we are solving the linearized gap equation.

Let us recall here that we are considering the case in which the pair condensate is color-antisymmetric and it is either a Lorentz scalar or a pseudo-scalar. This forces $K_{s(\text{ps})}^{fg}(0)$ to be antisymmetric under the exchange of flavor indices $f \leftrightarrow g$ due to the anti-commuting nature of the fermion fields. Such condensates can be decomposed as $K_{s(\text{ps})}^{fg}(0) = a_1 t_1^{fg} + a_3 t_3^{fg} + a_{13} \omega_{13}^{fg} + a_{24} \omega_{24}^{fg} + a_{25} (t_2 t_5)^{fg} + a_{45} (t_4 t_5)^{fg}$, where we have introduced the six independent anti-symmetric

matrices $t_1, t_3, \omega_{13}, \omega_{24}, t_2t_5,$ and t_4t_5 , with $t_\mu = \gamma_\mu, \omega_{\mu\nu} = (i/2)[t_\mu, t_\nu]$, and $t_5 = t_1t_2t_3t_4$. We have used the representation for the Dirac gamma matrices given by

$$\gamma_i = \begin{pmatrix} 0 & i\sigma^i \\ -i\sigma^i & 0 \end{pmatrix}, \quad \gamma_4 = \begin{pmatrix} I_2 & 0 \\ 0 & -I_2 \end{pmatrix},$$

where σ^i represent the Pauli matrices and I_2 represents the 2×2 identity matrix.

We calculate the coefficients $a_{1,3,13,24,25,45}$ numerically from the obtained eigenvector and find $|a_{13}|/a_{\text{sum}} > 0.997$ in $K_s^{fg}(0)$ and $|a_{24}|/a_{\text{sum}} > 0.997$ in $K_{\text{ps}}^{fg}(0)$, where $a_{\text{sum}} = \sum_{i=1,3,13,24,25,45} |a_i|$. This result suggests the following structures

$$K_s^{fg}(n) = \omega_{13}^{fg} \kappa_s(n), \quad (6)$$

$$K_{\text{ps}}^{fg}(n) = \omega_{24}^{fg} \kappa_{\text{ps}}(n), \quad (7)$$

with the flavor-independent coefficients $\kappa_{s(\text{ps})}(n)$, which give the spatial structure.

Let us discuss the implications of the flavor structure (6) and (7). Note first that the chiral $SU_L(4) \times SU_R(4)$ symmetry of the continuum theory is reduced on the lattice to the chiral $U(1)$ symmetry $\psi(n) \rightarrow e^{i\theta\gamma_5 \otimes t_5} \psi(n)$ in the case of the massless staggered fermions. Whether this symmetry is spontaneously broken or not depends on the flavor structure of the condensate. Under the infinitesimal chiral $U(1)$ transformation, Eq. (5) becomes

$$K_{s(\text{ps})}^{fg}(n) \rightarrow K_{s(\text{ps})}^{fg}(n) + i\theta \left(\sum_{f'} t_5^{ff'} K_{\text{ps}(s)}^{f'g}(n) + \sum_{g'} K_{\text{ps}(s)}^{fg'}(n) t_5^{gg'} \right). \quad (8)$$

When $K_s^{fg}(n)$ and $K_{\text{ps}}^{fg}(n)$ have the structure (6), (7), we therefore obtain

$$K_{s(\text{ps})}^{fg}(n) \rightarrow K_{s(\text{ps})}^{fg}(n) + 2i\theta\omega_{13(24)}^{fg} \kappa_{\text{ps}(s)}(n) \quad (9)$$

by using $\omega_{13t_5} = \omega_{24}$ and $\omega_{24t_5} = \omega_{13}$, which implies that the chiral $U(1)$ symmetry is broken spontaneously. This is in contrast to the other patterns $K_{s(\text{ps})}(n) \sim t_1, t_3, t_2t_5, t_4t_5$ since they are invariant under the chiral $U(1)$ transformation as one can show by using Eq. (8). Note that there is another possibility for condensate $K_s^{fg}(n) = \omega_{24}^{fg} \kappa_s(n)$ and $K_{\text{ps}}^{fg}(n) = \omega_{13}^{fg} \kappa_{\text{ps}}(n)$ that breaks the chiral $U(1)$ symmetry spontaneously. Thus, our method is capable of determining not only the symmetry breaking pattern but also the actual structure of the Cooper pairs thanks to the fact that we do not have to impose any ansatz on it.

We also investigate the spatial structure of the Cooper pairs represented by $\kappa_{s(\text{ps})}(n)$. For that, it is convenient to consider the momentum representations $\tilde{\kappa}_{s(\text{ps})}(p)$. Figure 3 shows the dependence of $\tilde{\kappa}_s(p)$ on the spatial momenta p_1 and p_2 for $p_3 = 0$ and the lowest Matsubara frequency $p_4 = \pi/L_t$ chosen at the position of the second peak. One can see that $|\tilde{\kappa}_s(p)|$ has relatively large values on the Fermi surface, which is represented by the blue line, and the values on the Fermi surface are almost the same. This clearly shows that the quarks on the Fermi surface form the Cooper pairs and they are spatially isotropic s-waves. Figure 3 (b) shows that all the modes on the Fermi surface have the same phase. This is consistent with the BCS theory of superconductivity, where the phase of the wave function is spatially aligned implying that the $U(1)$ particle-number symmetry is spontaneously broken. The results for $\tilde{\kappa}_{\text{ps}}(p)$ are qualitatively the same as those for $\tilde{\kappa}_s(p)$.

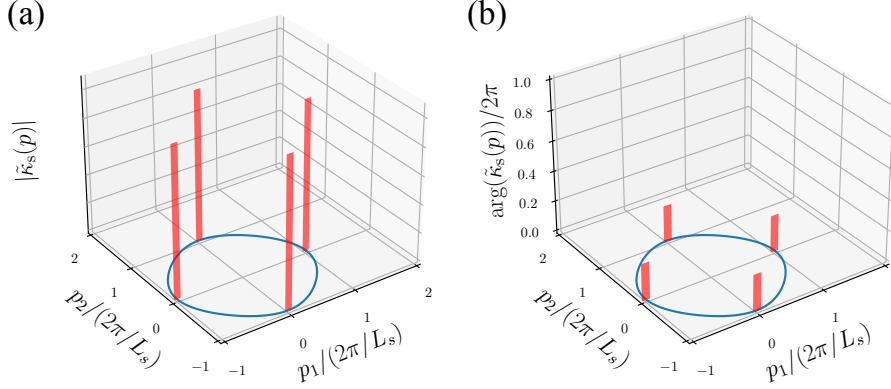


Figure 3: The p_1 and p_2 dependence of $\tilde{\kappa}_s(p)$ is shown for $p_3 = 0$ and $p_4 = \pi/L_t$ with $m = 0$ and $\mu = \sinh^{-1}(\sin(2\pi/L_s))$. Figure (a) shows the absolute value $|\tilde{\kappa}_s(p)|$ in arbitrary units, whereas Fig. (b) shows the phase $\arg(\tilde{\kappa}_s(p))$ for the momentum p at which $|\tilde{\kappa}_s(p)|$ has large values. The blue line represents the Fermi surface for $p_3 = 0$.

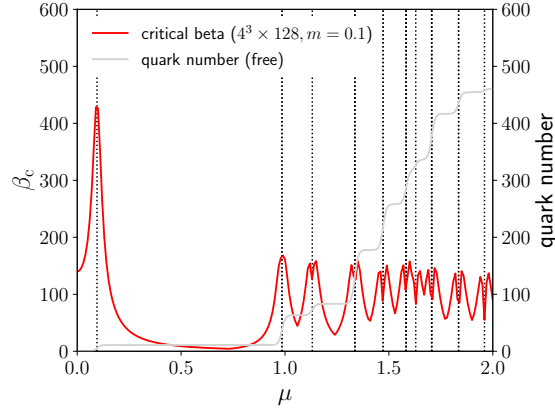


Figure 4: The critical coupling β_c is plotted as a function of μ for the Wilson fermions on a $4^3 \times 128$ lattice. The gray solid line represents the quark number in the free case, whereas the vertical black dotted lines represent the position of the energy levels of free quarks.

5. Critical coupling for the Wilson fermions

It is expected that various types of CSC appear depending on the number of flavors. An advantage of the Wilson fermions to the staggered fermions is that one can choose the number of flavors freely, although the drawback is that one loses explicit chiral symmetry. Figure 4 shows the result for the critical coupling β_c with the lattice size $4^3 \times 128$ and $m = 0.1$. The result does not depend on the number of flavors except for the one-flavor case, which should be treated in a different manner since the anti-symmetric flavor structure is not possible. We also show the particle number of quarks N_q in the free case by the gray solid line and the position of the quark energy levels by the black vertical lines. As in the case of the staggered fermions, we can see peaks in β_c corresponding to the jumps of N_q at the energy levels. On the other hand, we observe more structures than in the

case of staggered fermions, such as splitting of the peaks at the energy levels higher than the third one. We are currently investigating the structure of the Cooper pairs to clarify the relation to the splitting of the peaks.

6. Conclusion

We have investigated color superconductivity (CSC) on the lattice based on perturbative calculations without any ansatz on the structure of the Cooper pairs. In our method, the critical coupling β_c is obtained by calculating the largest eigenvalue of the matrix that appears in the linearized gap equation, which is feasible on a finite lattice. By applying this method to the staggered fermions, we have obtained β_c as a function of the chemical potential μ , which gives the parameter region for CSC. The result shows that β_c has peaks at μ corresponding to the quark energy levels. We have also investigated the structure of the Cooper pairs at the critical point from the eigenvector corresponding to β_c in the massless case. It turns out that the flavor structure of the (pseudo) scalar condensate thus specified breaks the chiral U(1) symmetry of the staggered fermions spontaneously. We have also obtained the results of β_c in the Wilson-fermion case, which show some splitting of the peaks in contrast to the staggered fermions.

In the staggered-fermion case, we have also investigated other types of condensates such as a pseudo-vector and a tensor as well as the effect of the quark mass on the Cooper pairs and the degeneracy of the largest eigenvalue, which shall be reported in the forth-coming paper. We hope that our prediction on the parameter region for CSC is useful in exploring the QCD phase diagram based on first-principles calculations. We also expect that the structure of the condensate provides useful information for the construction of the order parameter to detect the CSC. We are currently trying to observe the CSC on the lattice by using the complex Langevin method (CLM). In order to explore the parameter regions suggested in the present work, we need to extend our previous study of dense QCD with the staggered fermions [10] to the case with small aspect ratios of the lattice size. The results for some candidate of the order parameter for the CSC are presented in Ref. [15]. As for the Wilson fermion, some basic properties of the CLM for $N_f = 2, 2 + 1, 3, 4$ on lattices with small aspect ratio are presented in Ref. [16].

Acknowledgments

T. Y. was supported by the RIKEN Special Postdoctoral Researchers Program. Y. N. was supported by JSPS KAKENHI Grant Number JP21K03553. J. N. was supported in part by JSPS KAKENHI Grant Number JP16H03988. S. T. was supported by the RIKEN Special Postdoctoral Researchers Program. Numerical computation was carried out on the Oakbridge-CX provided by the Information Technology Center at the University of Tokyo through the HPCI System Research project (Project ID: hp200079, hp210078) and the Yukawa Institute Computer Facility.

References

- [1] G. Parisi, *Physics Letters B* **131**, 393 (1983).
- [2] J. R. Klauder, *Phys. Rev. A* **29**, 2036 (1984).

- [3] C. E. Berger, L. Rammelmüller, A. C. Loheac, F. Ehmman, J. Braun, and J. E. Drut, *Phys. Rept.* **892**, 1 (2021).
- [4] B. C. Barrois, *Nuclear Physics B* **129**, 390 (1977).
- [5] S. C. Frautschi, *Asymptotic Freedom and Color Superconductivity in Dense Quark Matter* (Springer US, Boston, MA, 1980), pp. 19–27.
- [6] D. Bailin and A. Love, *Nuclear Physics B* **190**, 175 (1981).
- [7] M. G. Alford, K. Rajagopal, and F. Wilczek, *Nucl. Phys. B* **537**, 443 (1999), arXiv:hep-ph/9804403.
- [8] K. Rajagopal and F. Wilczek, *The Condensed matter physics of QCD* (, 2000), pp. 2061–2151, arXiv:hep-ph/0011333.
- [9] M. G. Alford, A. Schmitt, K. Rajagopal, and T. Schäfer, *Rev. Mod. Phys.* **80**, 1455 (2008).
- [10] Y. Ito, H. Matsufuru, Y. Namekawa, J. Nishimura, S. Shimasaki, A. Tsuchiya, and S. Tsutsui, *JHEP* **10**, 144 (2020), arXiv:2007.08778.
- [11] Y. Nambu, *Phys. Rev.* **117**, 648 (1960).
- [12] D. J. Thouless, *Annals of Physics* **10**, 553 (1960).
- [13] P. Amore, M. C. Birse, J. A. McGovern, and N. R. Walet, *Phys. Rev. D* **65**, 074005 (2002).
- [14] H. J. Rothe, *Lattice Gauge Theories*, 4th ed. (WORLD SCIENTIFIC, 2012), <https://www.worldscientific.com/doi/pdf/10.1142/8229>.
- [15] S. Tsutsui, Y. Ito, H. Matsufuru, Y. Namekawa, J. Nishimura, A. Tsuchiya, and T. Yokota, *PoS LATTICE2021*, 533 (2021).
- [16] Y. Namekawa, Y. Ito, H. Matsufuru, J. Nishimura, A. Tsuchiya, S. Tsutsui, and T. Yokota, *PoS LATTICE2021*, 623 (2021).